Seasonal cycle of oceanic CO2 from the sea ice edge to island blooms in the Scotia Sea, Southern Ocean

Jones, Elisabeth Marie; Bakker, D.C.E.; Venables, Hugh; Hugh, J; Hardman-Mountford, N. J.

Published in:
Marine Chemistry

DOI:
10.1016/j.marchem.2015.06.031

Publication date:
2015

Marine Chemistry 177 (2015) 490–500

Contents lists available at ScienceDirect

Marine Chemistry

journal homepage: www.elsevier.com/locate/marchem

Seasonal cycle of CO_2 from the sea ice edge to island blooms in the Scotia Sea, Southern Ocean

Elizabeth M. Jones [a,b,*], Dorothee C.E. Bakker [b], Hugh J. Venables [c], Nick J. Hardman-Mountford [d]

[a] Centre for Energy and Environmental Sciences, Energy and Sustainability Research Institute Groningen, University of Groningen, Nijenborgh 4, 9747 AG, Groningen, The Netherlands
[b] Centre for Ocean and Atmospheric Sciences, School of Environmental Sciences, University of East Anglia, Norwich NR4 7TJ, UK
[c] British Antarctic Survey, High Cross, Madingley Road, Cambridge CB3 0ET, UK
[d] Oceans and Atmosphere Flagship, Commonwealth Scientific and Industrial Research Organisation, Floreat, WA 6014, Australia

ARTICLE INFO

Article history:
Received 21 January 2015
Received in revised form 28 June 2015
Accepted 30 June 2015
Available online 4 July 2015

Keywords:
Oceanic carbon dioxide
Scotia Sea, Southern Ocean
Sea ice
South Georgia bloom
Biological carbon uptake

ABSTRACT

The Scotia Sea region contains some of the most productive waters of the Southern Ocean. It is also a dynamic region through the interaction of deep water masses with the atmosphere. We present a first seasonally-resolved time series of the fugacity of CO_2 (fCO_2) from spring 2006, summer 2008, autumn 2009 and winter (potential temperature minimum) along a 1000 km transect from the pack ice to the Polar Front to quantify the effects of biology and temperature on oceanic fCO_2. Substantial spring and summer decreases in sea surface fCO_2 occurred in phytoplankton blooms that developed in the naturally iron-fertilised waters downstream (north) of South Georgia island (54–55°S, 36–38°W) and following sea ice melt (in the seasonal ice zone). The largest seasonal fCO_2 amplitude (ΔfCO_2) of −159 μatm was found in the South Georgia bloom. In this region, biological carbon uptake dominated the seasonal signal, reducing the winter maxima in oceanic fCO_2 by 257 μatm by the summer. In the Weddell–Scotia Confluence, the southern fringe of the Scotia Sea, the shift from wintertime CO_2-rich conditions in ice covered waters to CO_2 undersaturation in the spring blooms during and upon sea ice melt created strong seasonality in oceanic fCO_2. Temperature effects on oceanic fCO_2 ranged from $\Delta fCO_{2\ sst}$ of ~55 μatm in the seasonal ice zone to almost double that downstream of South Georgia (98 μatm). The seasonal cycle of surface water fCO_2 in the high-nutrient low-chlorophyll region of the central Scotia Sea had the weakest biological control and lowest seasonality. Basin-wide biological processes dominated the seasonal control on oceanic fCO_2 ($\Delta fCO_{2\ bio}$ of 159 μatm), partially compensated (43%) by moderate temperature control ($\Delta fCO_{2\ sst}$ of 68 μatm). The patchwork of productivity across the Scotia Sea creates regions of seasonally strong biological uptake of CO_2 in the Southern Ocean.

1. Introduction

The Southern Ocean plays a key role in the global carbon cycle through the interaction of upper ocean processes with atmospheric carbon dioxide (CO_2) and the ventilation of deep waters (Watson and Orr, 2003; Naveira Garabato et al., 2004; Takahashi et al., 2009). However, oceanic CO_2 data are sparse in the Southern Ocean and the magnitude and variability of seasonal and annual atmospheric CO_2 uptake remain relatively unknown compared to other areas of the global ocean (Metzl et al., 2006; Lenton et al., 2013; Landschützer et al., 2014). The Scotia Sea, in the Atlantic sector of the Southern Ocean, is an important component of the overturning circulation (Locarnini et al., 1993; Naveira Garabato et al., 2002, 2004; Meredith et al., 2008). The small ocean basin encompasses diverse Southern Ocean ecosystems, from a seasonal ice zone to oceanic islands, where the movement of major water masses and presence of fronts of the Antarctic Circumpolar Current (ACC) generates rich biological diversity (Holm-Hansen et al., 2004; Murphy et al., 2007) and extensive biogeochemical cycling. Sea ice covers the southern Scotia Sea during winter and has a variable northward extent into the central part of the basin. The seasonal advance and retreat of sea ice coupled with frontal meandering induces connective biogeochemical pathways from southern regions (e.g., the Weddell Sea and Antarctic Peninsula), to the north (Murphy et al., 2007) contributing to the basin-wide biological diversity (Atkinson et al., 2001; Meredith et al., 2008). Limited data in the region have revealed that the patchwork of productivity creates areas of contrasting sea surface CO_2 concentrations, from spring and summer CO_2 supersaturation in largely un-productive waters and beneath sea ice cover (Shim et al., 2006; Jones et al., 2012) to substantial biological carbon uptake within intense seasonal blooms (Jones et al., 2010, 2012). The large blooms in the Scotia Sea region can contribute to sequestration of atmospheric CO_2 and export of carbon to the deep ocean (Schlitzer, 2002; Pollard et al., 2009; Takahashi et al., 2009; Korb et al., 2012).

* Corresponding author at: Centre for Energy and Environmental Sciences, Energy and Sustainability Research Institute Groningen, University of Groningen, Nijenborgh 4, 9747 AG, Groningen, The Netherlands.
E-mail address: e.m.jones@rug.nl (E.M. Jones).

http://dx.doi.org/10.1016/j.marchem.2015.06.031
0304-4203/

The Scotia Sea is bound to the north, south and east by the Scotia Ridge, a sub-marine arc with island protrusions at the South Orkney Islands, on the South Scotia Ridge, and the island of South Georgia on the North Scotia Ridge (Fig. 1). It is a dynamic region due to the ventilation and mixing of water masses in the ACC through the interactions with rugged bathymetry and wind stress (Naveira Garabato et al., 2004). The ACC is split by a series of frontal jets, which are identified, from north to south, as the Sub-Antarctic Front (SAF), Polar Front (PF), the Southern ACC Front (SACCF) and the Southern Boundary (SB) (Orsi et al., 1995). The Polar Front passes through the western part of the Scotia Sea and leaves the Scotia Sea for the Georgia Basin across the North Scotia Ridge (Smith et al., 2010; Venables et al., 2012). The SACCF passes through the central Scotia Sea before retroflecting around the eastern shelf of the North Scotia Ridge and into the Georgia Basin (Trathan et al., 1997; Thorpe et al., 2002). Mesoscale activity associated with the SACCF can lead to variability in hydrographic and biogeochemical parameters across the Scotia Sea (Boehme et al., 2008; Whitehouse et al., 2012), with the front located in close proximity (~50 km) to the SB (Venables et al., 2012). Circumpolar Deep Water upwells and outcrops at the surface towards the southern limit of the ACC at the SACCF and SB (Orsi et al., 1995; Pollard et al., 2002; Boehme et al., 2008). The SB is the southernmost front in the region and marks the limit of the ACC and the boundary of the Weddell–Scotia Confluence, a transition zone between the Scotia Sea to the north and Weddell Sea to the south as waters flow off the tip of the Antarctic Peninsula and from the Weddell Sea and infiltrate the ACC (Patterson and Sievers, 1980; Whitworth et al., 1994; Meredith et al., 2008; Jullion et al., 2014).

A wide range of productivity regimes occur across the Scotia Sea against a back-drop of high-nutrient low-chlorophyll (HNLC) conditions common to much of the remote Southern Ocean (Park et al., 2010; Whitehouse et al., 2012). Some of the longest lasting phytoplankton blooms in the ACC develop annually in the Georgia Basin, downstream (north) of the island of South Georgia (Atkinson et al., 2001; Korb and Whitehouse, 2004; Borrione and Schlitzer, 2013). Natural enrichment of the limiting micronutrient iron can occur from South Georgia, shelves and shallow sediments of the North Scotia Ridge (Holeton et al., 2005; Nielsdóttir et al., 2012), promoting high atmospheric CO_2 uptake (Jones et al., 2012). In the seasonal ice zone, blooms are frequently linked to the retreat of the ice edge (Lancelot et al., 1993; Nielsdóttir et al., 2012) and create transient and substantial CO_2 sinks (Jones et al., 2010). By contrast, the central Scotia Sea displays considerable spatial and temporal variability in phytoplankton biomass, where extensive blooms in one year can be followed by near-HNLC conditions in the next (Whitehouse et al., 2008, 2012; Park et al., 2010; Korb et al., 2012). Alleviation of HNLC conditions is through iron enrichment (de Baar et al., 1995; Boyd et al., 2007) under favourable light conditions, where iron sources to surface waters in the Scotia Sea include interaction of the ACC with shallow topography, e.g., the Scotia Arc (Korb and Whitehouse, 2004; Holm-Hansen et al., 2004; Meskhidze et al., 2007; Nielsdóttir et al., 2012), melting sea ice (de Baar and de Jong, 2001; Nielsdóttir et al., 2012) and advection within the SACCF and SB from an upstream source, e.g., the Shackleton Fracture Zone and Antarctic Peninsula shelf (Ardelan et al., 2010; Zhou et al., 2010).

The dynamic hydrographic and biological regimes of the Scotia Sea create a natural 'mesocosm' to investigate the seasonal cycle of oceanic CO_2. Quantifying the processes that control the cycling of CO_2 across several typical Southern Ocean environments is fundamental to better determine the role of the polar oceans in the global carbon cycle. While the biological and biogeochemical processes highlighted in the preceding paragraph have been described, the quantification of their influence on CO_2 dynamics in the Scotia Sea region is limited to a few localised observations in spring and summer (Shim et al., 2006; Jones et al., 2012). This study resolves for the first time the relative contribution of biological and physical (principally temperature) controls as drivers of variability in oceanic CO_2 across the Scotia Sea between different seasons. We present a new time series of oceanic CO_2 from an ~1000 km meridional transect during spring 2006, summer 2008, autumn 2009 and winter (potential temperature minimum). Data extend from the seasonal pack ice in the Weddell–Scotia Confluence to the large phytoplankton blooms downstream (north) of South Georgia and up to the Polar Front. The oceanic context is set by considering the basin-scale spatial and temporal distribution and variability of phytoplankton blooms and sea ice cover, as determined by satellite measurements during the 2006–2009 study period. Finer resolution shipboard measurements of hydrographic variables, macronutrients and chlorophyll-a are considered to identify the physical (temperature, salinity, sea ice cover, mixed layer depth) and biological controls that drive the seasonal variability oceanic CO_2 in the Scotia Sea. The data highlight the seasonal dynamics as key to understanding the carbon cycle of the polar oceans.

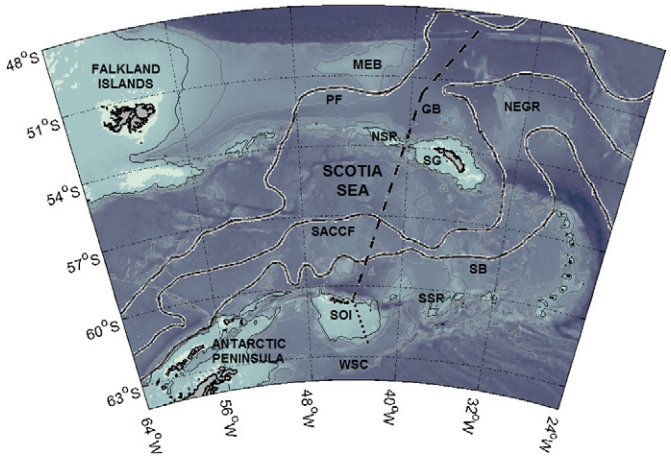

Fig. 1. Map of the Scotia Sea showing the location of the seasonal meridional transect by large dashed line and summer 2008 extension as a dotted line. Important topographic features are: South Scotia Ridge (SSR), South Orkney Islands (SOI), South Georgia (SG), North Scotia Ridge (NSR), Georgia Basin (GB), Northeast Georgia Rise (NEGR) and Maurice Ewing Bank (MEB). The location of the Weddell–Scotia Confluence (WSC) is also marked. Schematic positions of the Southern Boundary (SB), Southern ACC Front (SACCF) and the Polar Front (PF) are shown, adapted from Meredith et al. (2003). Depth contours are at 1000 and 2000 m (GEBCO, 2001).

2. Methods

2.1. Oceanographic sampling

Data were collected in the Scotia Sea, Atlantic sector of the Southern Ocean, during three cruises onboard RRS *James Clark Ross* in spring, summer and autumn of consecutive years as part of the British Antarctic Survey DISCOVERY-2010 programme (Tarling et al., 2012). An ~1000 km meridional transect that extended from south of the South Orkney Islands to the Polar Front (Fig. 1) was occupied during austral (1) spring (JR161; 24.10.06–02.12.06), (2) summer (JR177; 31.12.07–14.02.08) and (3) autumn (JR200; 12.03.09–15.04.09). The depth of the mixed layer is defined as the depth at which the potential density exceeds that measured at 10 m by 0.05 kg m^{-3} (Brainerd and Gregg, 1995). Mixed layer depths (mld) were determined from 2 dbar resolution depth profiles of the conductivity, temperature, and depth (CTD) sensor (Seabird 911+) deployment at each hydrographic station (Venables et al., 2012). Positions of the SB, SACCF and PF are expressed as latitudinal ranges based on absolute dynamic sea-surface height during each cruise (Venables et al., 2012). Sea surface temperature and salinity data were obtained from the underway seawater supply (Oceanlogger SeaBird Electronics SBE45 CTD) with an intake at 6.5 m depth. Salinity values are reported on the practical salinity scale. Samples for chlorophyll-a analysis (200–500 mL) were filtered through glass fibre filters (0.7 μm

poresize GF/F, Fisherbrand), frozen at −20 °C and then extracted into 10 mL 90% acetone for 24 h before analysis on a fluorometer (Turner Designs TD-700). A detailed description of the chlorophyll-a method is presented in Korb and Whitehouse (2004).

2.2. Sea surface CO_2

2.2.1. Seasonal observations and CO_2 disequilibrium

Measurements of the fugacity of CO_2 (fCO_2) in seawater and air were made during each cruise using a PML/Dartcom Live CO_2 system (Hardman-Mountford et al., 2008), based on principles outlined in Cooper et al. (1998). The CO_2 disequilibrium (ΔfCO_2) is the difference between the fCO_2 in surface water and overlying air, where negative values represent CO_2 undersaturation with respect to the atmosphere. Atmospheric samples were taken from an inlet located forward at 15 m height of the RRS *James Clark Ross*. Mixing ratios of CO_2 and water were determined by infra-red detection with a LI-COR 840. The LI-COR was calibrated using secondary gas standards with nominal CO_2 concentrations of 250 ppm and 450 ppm in artificial air and nitrogen was the zero reference gas. All gases underwent pre- and post-cruise calibration against certified primary standards from the National Oceanic and Atmospheric Administration (NOAA) at Plymouth Marine Laboratory. Samples from the equilibrator headspace and marine air were partially dried in a condenser prior to analysis in the LI-COR. The fCO_2 was computed from the mixing ratios and the ship's barometric pressure and then corrected for seawater vapour pressure (Weiss and Price, 1980). Two platinum resistance thermometers located in the upper and lower part of the equilibrator determined the average warming (all measurements) of the seawater between the intake and the equilibrator as 0.6 °C ($\sigma = 0.3$ °C; $n = 3568$). Sea surface fCO_2 data were corrected to sea surface temperature to account for this warming (Takahashi et al., 1993). The accuracy of the fCO_2 data is determined at 3 μatm from an instrument intercomparison carried out during cruise JR177 (Jones, 2010). The precision is estimated as better than 2 μatm.

Concentrations of dissolved inorganic carbon and alkalinity were measured during summer 2008 (cruise JR177) at the depth of the potential temperature minimum (θ_{min}) for each hydrographic station; a full description of sample collection, analysis and data is presented in Jones et al. (2012). The potential temperature minimum represents the Winter Water (Jennings et al., 1984), the remnant of the mixed layer from the preceding winter, i.e., 2007. Parameters measured in the Winter Water during summer 2008 are taken to reflect surface conditions during winter 2007 and were used to calculate sea surface fCO_2 with the CO2Sys programme (Lewis and Wallace, 1998; van Heuven et al., 2011) using thermodynamic dissociation constants for K_1 and K_2 by Mehrbach et al. (1973), re-fitted by Dickson and Millero (1987). The accuracy of calculated fCO_2 is better than 6 μatm (Millero, 1995). Thus, winter (θ_{min}) fCO_2 data is used to complement the spring 2006, summer 2008 and autumn 2009 sea surface fCO_2 seasonal time series.

2.2.2. Biological and physical CO_2 signals

The seasonal changes in sea surface fCO_2 can be separated into biological and physical (temperature) signals (Takahashi et al., 2002). Other processes affecting oceanic CO_2, such as air–sea CO_2 exchange, advection, mixing, upwelling and changes in alkalinity, e.g., from calcium carbonate precipitation (calcification) and dissolution, are not accounted for independently here and are incorporated into the 'biological' signal. To remove the effects of temperature, sea surface fCO_2 data measured at observed temperature (sst_{obs}) are normalised to the average sea surface temperature (sst_{ave}, 1.52 °C) of spring, summer, autumn and winter (θ_{min}) along the transect:

$$fCO_2 \text{ at } sst_{ave} = fCO_2 \text{ at } sst_{obs} \times \exp(0.0423(sst_{ave} - sst_{obs})). \quad (1)$$

The temperature signal in sea surface fCO_2 is determined from the mean fCO_2 of spring, summer, autumn and winter ($fCO_{2\ ave}$) along the transect and the difference between sst_{obs} and sst_{ave}:

$$fCO_2 \text{ at } sst_{obs} = fCO_{2\ ave} \times \exp(0.0423(sst_{obs} - sst_{ave})). \quad (2)$$

This approach assumes that the observed field data cover the maxima and minima of the seasonal variations in sea surface temperature and fCO_2, which has limitations for this basin-wide study with large spatial variability. This is addressed here by using data at the temperature minimum (as a proxy for winter sea surface data) and by interpreting the seasonal changes (amplitudes) within a wider context set by satellite data. Seasonal amplitudes in oceanic fCO_2 due to biological ($\Delta fCO_{2\ bio}$) and temperature ($\Delta fCO_{2\ sst}$) effects are obtained from the difference between the maximum and minimum values in fCO_2 at sst_{ave} and fCO_2 at sst_{obs}, respectively, from all spring 2006, summer 2008, autumn 2009 and winter (θ_{min}) data:

$$\Delta fCO_{2\ bio} = (fCO_2 \text{ at } sst_{ave})_{max} - (fCO_2 \text{ at } sst_{ave})_{min} \quad (3)$$

$$\Delta fCO_{2\ sst} = (fCO_2 \text{ at } sst_{obs})_{max} - (fCO_2 \text{ at } sst_{obs})_{min}. \quad (4)$$

The influence of the biological and temperature controls on seawater fCO_2 is investigated by comparison of the difference ($\Delta fCO_{2\ sst} - \Delta fCO_{2\ bio}$) and ratio ($\Delta fCO_{2\ sst}/\Delta fCO_{2\ bio}$) of the two expressions. In regions of high biological activity and/or strong seasonal variability in biological activity the difference ($\Delta fCO_{2\ sst} - \Delta fCO_{2\ bio}$) is negative and the ratio ($\Delta fCO_{2\ sst}/\Delta fCO_{2\ bio}$) is less than 1. In regions of low biological activity and/or weak seasonal variability in biological activity the difference is positive and the ΔfCO_2 ratio is greater than 1 (Thomas et al., 2005).

2.3. Satellite chlorophyll-a and sea ice cover

Satellite ocean colour from SeaWiFS (2006–2007) and MODIS-Aqua (2006–2009) were obtained from http://oceancolor.gsfc.nasa.gov/ (July 2009) as 8 day, 9 km level 3 mapped data (Feldman and McClain, 2006a, b). Satellite derived concentrations of chlorophyll-a (chl-a) are used as an indicator of spatio-temporal variation in phytoplankton biomass. Bloom conditions are defined as having chlorophyll-a concentrations exceeding 0.75 mg chl-a m^{-3} (Korb et al., 2012) and HNLC conditions as less than 0.2 mg m^{-3} in the presence of high macronutrient concentrations (Whitehouse et al., 2012). The 8 day composite images were used to determine the initiation and termination of the blooms. Bloom progression could be more easily tracked using the multi-day composites rather than daily images, which were strongly affected by cloud cover. The multi-day composites maintained a sufficient temporal resolution.

Sea ice concentration data at 4 km resolution were obtained through the Operational Sea Surface Temperature and Sea Ice Analysis (OSTIA) service (http://ghrsst-pp.metoffice.com/pages/latest_analysis/ostia.html; December 2009), part of the Group for High-Resolution Sea Surface Temperature (Stark et al., 2007). The ice edge is defined here as the terminus of consolidated sea ice along the transect, expressed as 0.5 fractional (50%) sea ice cover during each seasonal cruise. The seasonal ice zone (SIZ) is the region between the maximum and minimum sea ice extent based on monthly fractional sea ice cover during the study period 2006–2009.

3. Results

3.1. Bloom dynamics: seasonal and year-to-year variations

The SeaWiFS and MODIS-Aqua time series (Fig. 2) shows high spatial and temporal variability in surface chlorophyll-a in the Scotia Sea (55–59.3°S, 25–55°W) and Georgia Basin (49.5–53.0°S, 25–45°W) regions throughout the 3-year study period. A general seasonal cycle can

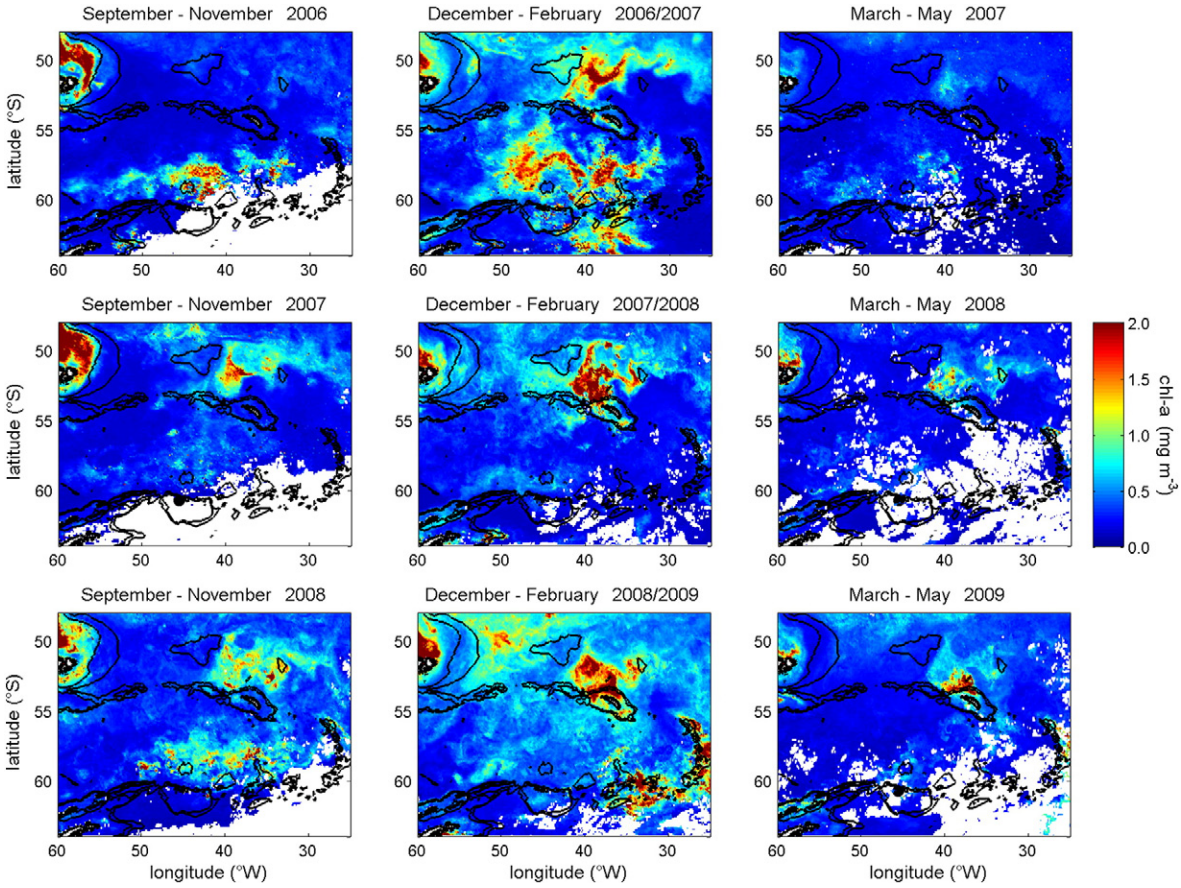

Fig. 2. Seasonal satellite chlorophyll-a (chl-a, mg m^{-3}) composite time series for the Scotia Sea region for each austral spring (September–November), summer (December–February) and autumn (March–May) during the 2006–2009 study period. Winter (June–August) images, mostly obscured by ice and/or cloud cover and data limited by reduced light availability, are not shown. Data are from 2006 (SeaWiFS/MODIS merged product), 2007 (SeaWiFS), 2008 (MODIS) and 2009 (MODIS). Depth contours are at 1000 and 2000 m (GEBCO, 2001).

be depicted: chlorophyll-a patches appeared during spring (September, October, November), sporadic chlorophyll-a maxima occurred in the southern and central Scotia Sea in both spring and summer, followed by peaks in the Georgia Basin in summer (December, January, February), in some years persisting until autumn (March, April, May). The northern Scotia Sea regularly exhibited HNLC-type characteristics as evident from sea surface nitrate and phosphate concentrations measured during each cruise, reported in Whitehouse et al. (2012). Sea ice obscured part of the southern basin from satellite detection during the winter, while shorter daylight hours also limited data coverage (June, July, August) (hence not shown in Fig. 2).

Each phytoplankton bloom in the Scotia Sea and the Georgia Basin is ranked in terms of areal extent and longevity to give a relative 'strength' as a product of these two features (Table 1). Blooms show high inter-annual variability in extent and duration in the Scotia Sea (Fig. 3) and seasonality. In 2006/2007 a huge bloom lasted for up to 6 months and extended across the central Scotia Sea (rank product 1) (Figs. 2 and 3). Extensive blooms in the Georgia Basin occur annually, often persisting for up to 6 months from spring until autumn, peaking in intensity during the summer (rank products 2, 3, 4).

3.2. The seasonal ice zone of the Scotia Sea

The seasonal advance and retreat of the sea ice from 2006 to 2009 can be observed from satellite derived sea ice cover to locate the position of the sea ice edge (Fig. 4). The ice typically originates in the Weddell Sea and drifts and extends northwards into the Scotia Sea during winter (Murphy et al., 1995). During February and March each year the region was consistently ice free. Inter-annual variation in the timing of the sea ice advance and retreat and maximum coverage is evident. The maximum extent of sea ice, defined as the northward limit of the sea ice cover where ice is present for the whole month, reached 57°S in September 2007; defining the northward limit of the seasonal ice zone (SIZ) for the 2006/2009 study period. Summer–autumn 2007/2008 had a short ice free period of only 2 months (February to March) in the Scotia Sea. This was followed by relatively early seasonal sea ice advance in April 2008, making 2007/2008 a relatively 'icy' period. By contrast, sea ice had largely retreated from the Scotia Sea by December 2008, thus 2008/2009 was relatively ice free.

3.3. Sub-regions of the Scotia Sea

Combining remotely sensed chlorophyll-a (Fig. 2) data with sea surface hydrographic and biogeochemical data (Fig. 5), macronutrient distributions (Whitehouse et al., 2012) and frontal boundaries (Orsi et al., 1995; Venables et al., 2012), eight sub-regions were distinguished along the meridional transect for the 2006–2009 study period:

1. Weddell–Scotia Confluence (WSC; 62.6–59.3°S) includes the southern limit of the transect; the coldest waters and those south of the ACC, i.e., south of the SB; main part of the SIZ annually.
2. Southern Boundary (SB; 59.3–57.7°S) defined as the southern limit of the ACC as observed from the disappearance of Circumpolar Deep Water in potential temperature profiles during each cruise; regularly within the SIZ.
3. Southern ACC front (SACCF; 57.7–57.2°S) defined as the southern extent of the sub-surface 1.8 °C potential temperature contour from

Table 1
Areal extent and duration of the principal Scotia Sea (S Sea) and Georgia Basin (GB) blooms for each austral spring (September–November), summer (December–February) and autumn (March–May) during the 2006–2009 study period. Areal extent (10^3 km^2) and duration (days) for blooms (chl-a exceeds 0.75 mg m^{-3}) are determined from SeaWiFS/MODIS composite 8-day images. Areal extent is defined as the seasonal maximum limit of chlorophyll values exceeding 0.75 mg m^{-3} within the Scotia Sea (55–59.3°S, 25–55°W) and Georgia Basin (49.5–53.0°S, 25–45°W). Duration is defined as the length of time a bloom is present in the images, in factors of 8 days up to a maximum of 88 days (i.e., the whole season). No blooms were detected during winter (June, July, August) 2006–2009. Each bloom is ranked in terms of extent (1 = largest area) and duration (1 = longest duration). The relative 'strength' of each bloom is expressed as a product of area and duration ranking. The average relative strength of all blooms is 52. The four strongest blooms are highlighted in bold. Timing of the seasonal meridional transects is indicated (*).

Season	Year/s	Location	Extent		Duration		Rank product
			10^3 km^2	Rank	Days	Rank	
Spring*	2006	S Sea	256	5	48	4	20
		GB	8	18	32	6	108
Summer	2006/2007	S Sea	463	1	88	1	**1**
		GB	279	4	88	1	**4**
Autumn	2007	S Sea	46	13	8	9	117
		GB	30	15	8	9	135
Spring	2007	S Sea	50	12	32	6	72
		GB	165	9	64	3	27
Summer*	2007/2008	S Sea	41	14	32	6	84
		GB	325	2	88	1	**2**
Autumn	2008	S Sea	26	17	16	8	136
		GB	83	11	72	2	22
Spring	2008	S Sea	210	6	72	2	12
		GB	182	8	72	2	16
Summer	2008/2009	S Sea	196	7	72	2	14
		GB	298	3	88	1	**3**
Autumn*	2009	S Sea	29	16	24	7	112
		GB	102	10	40	5	50

potential temperature profiles during each cruise; regularly within the SIZ.

4. HNLC waters (57.2–56.0°S) defined by persistent high concentrations of nitrate and phosphate of 25–30 mmol m^{-3} and 1.5–2.0 mmol m^{-3} (Whitehouse et al., 2012), respectively. Chlorophyll-a concentrations are often less than 0.2 mg m^{-3} as determined from satellite and shipboard measurements; rarely within the SIZ.
5. Northern Scotia Sea (nSS; 56.0–55.0°S) defined as deep (>3000 m) waters up to the North Scotia Ridge; north of the SIZ.
6. North Scotia Ridge (NSR; 55.0–53.0°S) defined as shelf waters (<3000 m) across the ridge.
7. Georgia Basin (GB; 53.0–50.5°S) defined as the deep (>3000 m) basin northwest of the island of South Georgia.
8. Polar Front (PF; 50.5–49.5°S) defined as the northern limit of the sub-surface potential temperature minimum as observed from potential temperature profiles during each cruise; represents the northern limit of the meridional transect.

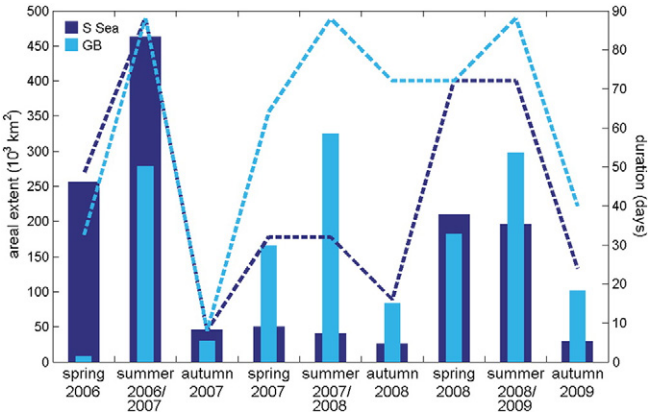

Fig. 3. Areal extent (10^3 km^2, bars) and duration (days, dashed lines) of the principal Scotia Sea (S Sea, dark blue) and Georgia Basin (GB, light blue) blooms for each austral spring (September–November), summer (December–February) and autumn (March–May) during the 2006–2009 study period (Table 1).

3.4. Seasonal CO_2 disequilibrium

The degree of CO_2 disequilibrium (ΔfCO_2) in seawater (Fig. 6) is regulated by biological production, temperature, salinity, sea ice cover and depth of the mixed layer. Temperature exerts a strong control on seawater fCO_2 (Fig. 7a) through changing the solubility of the gas in seawater (Weiss and Price, 1980). A normalisation of the seasonal fCO_2 time series to mean sea surface temperature has been made to remove the effects of temperature, following the empirical relationship of Takahashi et al. (2002).

Seasonal seawater fCO_2 minima in spring and summer are due to photosynthetic CO_2 uptake in phytoplankton blooms upon retreat of sea ice and in the naturally iron-fertilised waters downstream (north) of South Georgia island (Fig. 7c). Springtime maximum (positive) and minimum (negative) CO_2 disequilibrium occurred at the southern end of the transect ~60°S (Fig. 6a). High CO_2 disequilibrium of 62 μatm in cold, saline and deep mixed layers (80 m) occurred beneath sea ice (sea ice fraction 0.5–1.0) present around the South Orkney Islands (Fig. 5). In contrast, CO_2 disequilibrium of −82 μatm at ~57.5°S coincided with high chlorophyll-a values of 7.9 mg m^{-3} (Fig. 5b) in cool, less saline and shallower mixed layer (50 m) surface waters (Fig. 5c–e); symptomatic of recent sea ice melt. Springtime surface water fCO_2 varied significantly with chlorophyll-a concentrations ($r^2 = 0.79$, $m = -12.9$, $p < 0.001$, $n = 46$) and salinity, an indicator of sea ice melt, ($r^2 = 0.56, m = 289.1, p < 0.001, n = 781$) (Fig. 7b–c). The location of the sea ice edge during spring was around 59°S (Fig. 5f). Seasonal mixed layers of 100–120 m (Fig. 5e) in the north Scotia Sea and the North Scotia Ridge had sea surface fCO_2 close to atmospheric values (Fig. 5a) with very low chlorophyll-a (Fig. 5b). At the northern limit of the springtime transect, CO_2 disequilibrium shifted to −50 μatm in relatively warm surface waters of the Georgia Basin and the PF, where chlorophyll-a values were around 2 mg m^{-3} (Fig. 5b).

The summertime distribution of fCO_2 was dominated by intense undersaturation in the Weddell–Scotia Confluence, northern Scotia Sea regions (nSS and NSR) and Georgia Basin (Figs. 5a, 6b). A swift transition from fCO_2 saturation to substantial undersaturation of −100 μatm in the Weddell–Scotia Confluence (Fig. 5a) coincided with the transformation from cold, salty waters beneath sea ice to less saline, stratified surface waters with chlorophyll-a values of 3.5 mg m^{-3} (Fig. 5b–d) upon extensive sea ice melt (Fig. 5f). These trends are reflected in significant summertime sea surface fCO_2 correlation with chlorophyll-a concentrations ($r^2 = 0.38$, $m = -13.8$, $p < 0.001$, $n = 180$) and salinity ($r^2 = 0.24$, $m = 117.2, p < 0.001, n = 714$) for all data (Fig. 7b–c). The summertime ice edge was located around 62°S (Fig. 5f). A summer minimum in fCO_2 undersaturation of −116 μatm was measured alongside very high concentrations of chlorophyll-a over 10 mg m^{-3} in the relatively warm, stratified waters of the Georgia Basin (Fig. 5). By contrast, the central Scotia Sea (SACCF and HNLC) was moderately supersaturated as CO_2 disequilibrium approached 20 μatm with deeper mixed layers of about 80 m in the presence of low chlorophyll-a (Fig. 5a–b and e).

Surface waters had a fCO_2 range between 310 μatm and 400 μatm for the entire transect during autumn (Figs. 5 and 7). Disequilibrium of CO_2 changed from oversaturation (20 μatm) in relatively warm and saline waters of the central Scotia Sea, sub-regions SACCF and HNLC (Fig. 7a–b) to undersaturation (−50 μatm) in the Georgia Basin, where waters were fresher and chlorophyll-a values were high at 5 mg m^{-3}. Such surface water patterns created a significant and moderately strong relationship between autumnal fCO_2 and salinity ($r^2 = 0.67$, $m = 111.36$, $p < 0.001$, $n = 684$). A second area of fCO_2 undersaturation (−40 μatm) and smaller chlorophyll-a peak (2.5 mg m^{-3}) occurred near the South Orkney Islands, contributing to a weak but significant trend between fCO_2 and

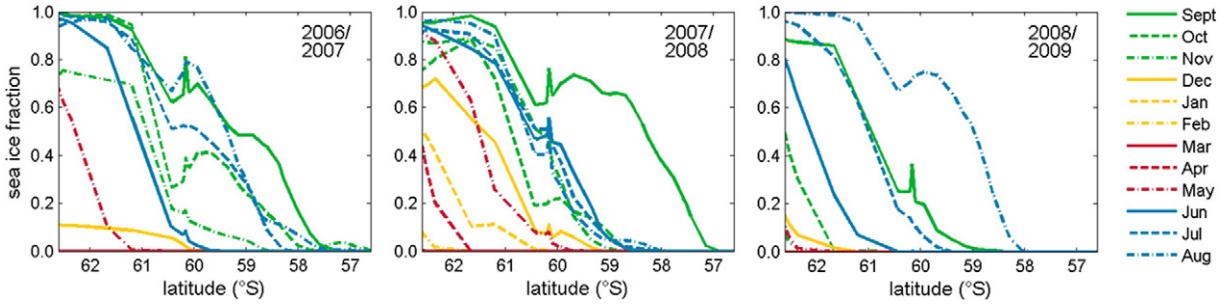

Fig. 4. Monthly satellite derived sea ice cover (fraction) along the meridional transect for the Scotia Sea and Weddell–Scotia Confluence from September to August 2006/2007, 2007/2008 and 2008/2009.

chlorophyll-a ($r^2 = 0.12$, $m = -8.9$, $p < 0.001$, $n = 131$) during the autumn (Fig. 7b–c).

Oceanic fCO_2 in Winter Water (θ_{min} data) indicate that sea surface fCO_2 during the winter is mostly supersaturated with respect to atmospheric CO_2 (Fig. 5a). High values between 380 and 450 μatm coincide with high salinities (>34.2) and low temperatures (<− 1.35 °C) beneath almost total ice cover in the Weddell–Scotia Confluence (Figs. 5 and 7). Winter sea surface fCO_2 maxima (440–455 μatm) occurred in deep mixed layers (120–130 m) in the Georgia Basin (Fig. 5). No winter data are available for the Polar Front region.

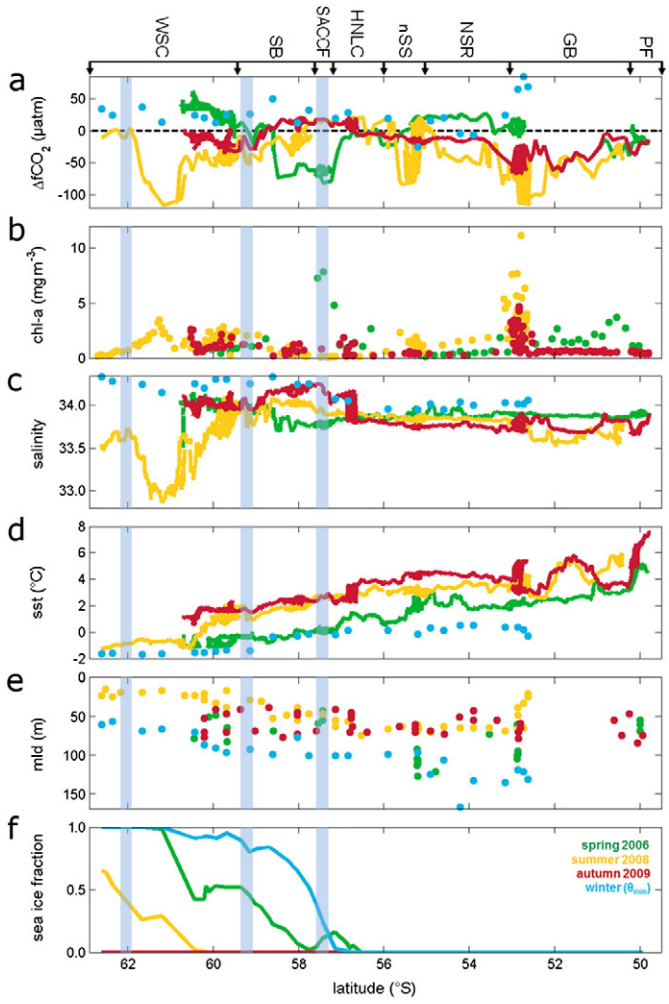

Fig. 5. The latitudinal distribution of sea surface (a) CO_2 disequilibrium (ΔfCO_2, μatm), (b) chlorophyll-a (chl-a, mg m^{-3}), (c) salinity, (d) sea surface temperature (sst, °C), (e) mixed layer depth (mld, m) and (f) sea ice cover (fraction) during spring 2006, summer 2008, autumn 2009 and winter (θ_{min}). The vertical grey bars mark the location of the sea ice edge in spring (~59°S), summer (~62°S) and winter (~57°S) as determined by the northern limit of 0.5 fractional sea ice cover in (f). The sea ice edge in autumn was located further south than the transect southern limit and is hence not shown. The latitudinal limits of the Weddell–Scotia Confluence (WSC), Southern Boundary (SB), Southern ACC Front (SACCF), high-nutrient low-chlorophyll (HNLC) waters, northern Scotia Sea (nSS), North Scotia Ridge (NSR), Georgia Basin (GB) and the Polar Front (PF) are indicated (black arrows).

The strongest seasonal biological signals ($\Delta fCO_{2\ bio}$) of 257 μatm and 196 μatm occurred in the Georgia Basin and Weddell–Scotia Confluence, respectively (Fig. 8a). This reflects the oceanic fCO_2 changes due to seasonal photosynthetic uptake of CO_2 in these regions. Temperature control ($\Delta fCO_{2\ sst}$) had comparatively little variation along the meridional transect with a slightly greater effect in the north compared to the south (Fig. 8a). Strong seasonal warming driving strong thermodynamic changes in oceanic CO_2 near the Polar Front has been previously observed along a south–north transect at 52°W in the Scotia Sea (Shim et al., 2006). The southern sub-regions lie within the seasonal ice zone where partial sea ice cover is still present during spring and summer (Fig. 4) and this reduces the time for sea surface warming. The northern sub-regions experience greater seasonal warming (Fig. 5d), where the maximum temperature control of 98 μatm occurred in the Georgia Basin (Fig. 8a). The HNLC waters in the central Scotia Sea displayed the lowest biological control of 97 μatm and weakest net seasonal variability of the whole region with a ΔfCO_2 ratio ($\Delta fCO_{2\ sst}/\Delta fCO_{2\ bio}$) of 0.7 (Fig. 8b).

4. Discussion

4.1. Strong CO_2 dynamics in the seasonal ice zone

Large seasonal fCO_2 amplitude is observed in the Weddell–Scotia Confluence through a synergy of weak temperature control ($\Delta fCO_{2\ sst}$), typical of the southern Scotia Sea, and strong biological CO_2 uptake ($\Delta fCO_{2\ bio}$) during the spring and summer sea ice thaw. The dominant seasonal biological control ($\Delta fCO_{2\ bio}$) of 196 μatm in the meltwaters of the Weddell–Scotia Confluence generated the substantial summertime CO_2 disequilibrium of around − 120 μatm, possibly with a minor contribution from calcium carbonate dissolution in the sea ice meltwater, respectively (Jones et al., 2010). For the whole SIZ (WSC, SB, SACCF), the distribution of sea surface fCO_2 displayed synchronicity to the seasonal transition from ice covered to ice free waters. The wintertime fCO_2 supersaturation in very cold, salty waters of the Weddell–Scotia Confluence is indicative of entrainment of CO_2 beneath sea ice. Throughout winter and early spring, remineralisation of organic matter, respiration, vertical mixing and brine rejection enable supersaturation of CO_2 beneath the pack ice (Nomura et al., 2006; Rysgaard et al., 2007). Ice covered waters of the Weddell–Scotia Confluence in spring were a potential source of CO_2 to the atmosphere as indicated by large, positive CO_2 disequilibrium. Breaking up of the sea ice near the South Orkney Islands could enable immediate release of the winter CO_2 'reserve' prior to springtime photosynthetic activity and biological

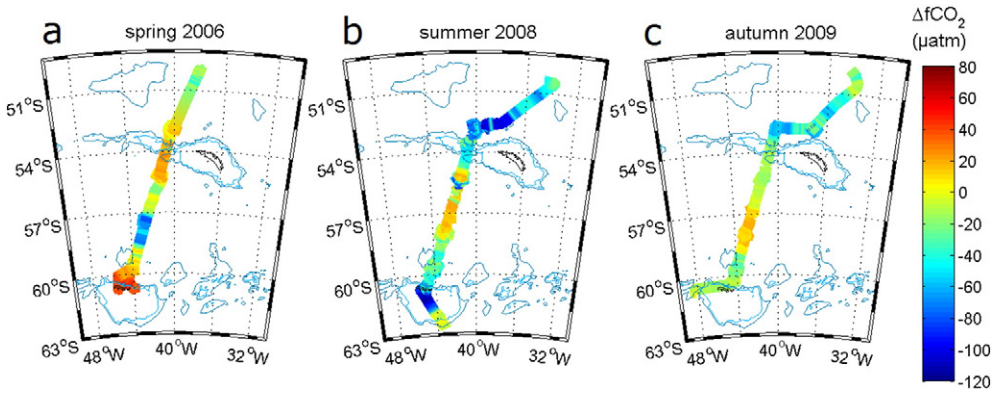

Fig. 6. Seasonal distribution of CO_2 disequilibrium (ΔfCO_2, μatm) along the meridional transect across the Weddell–Scotia Confluence, Scotia Sea and Georgia Basin during (a) spring 2006, (b) summer 2008 and (c) autumn 2009. Bathymetry contours as for Fig. 4.

CO_2 drawdown that occurs during and after sea ice melt (Bakker et al., 2008; Jones et al., 2010).

The shift from CO_2 saturation to undersaturation in close proximity aligns with the retreating seasonal ice edge, where phytoplankton blooms developed and strong CO_2 disequilibrium appeared to 'track' the southward retreating ice edge. Thawing sea ice led to stronger stratification and reduced surface ice cover, thus exposing algal cells to increased light levels alongside potential additional iron inputs. Iron might originate from melting sea ice (Sedwick and DiTullio, 1997; Nielsdóttir et al., 2012), shallow sediments from local sources such as the South Orkney Islands (Nielsdóttir et al., 2012), or upstream sources, e.g., the shelf of the Antarctic Peninsula (Hewes et al., 2008; Ardelan et al., 2010; Dulaiova et al., 2009). Iron (re)-supply to the central Scotia Sea could also result from upwelling of deep waters following water mass–topography interactions, e.g., the Antarctic Peninsula; melting sea ice and icebergs and subsequent transport eastwards within the SACCF (Sokolov and Rintoul, 2007; Dulaiova et al., 2009; Ardelan et al., 2010; Zhou et al., 2010; Venables et al., 2012). The large transit time from an upstream source to bloom location enables biological assimilation of the iron and physical dispersion, accounting for the temporal relief from iron stress and relatively short-lived blooms in the central Scotia Sea region (Korb et al., 2012; Whitehouse et al., 2012). Consumption of the reserve of macronutrients was evident within the diatom-cryptophyte blooms that were observed in spring 2006 (Korb et al.,

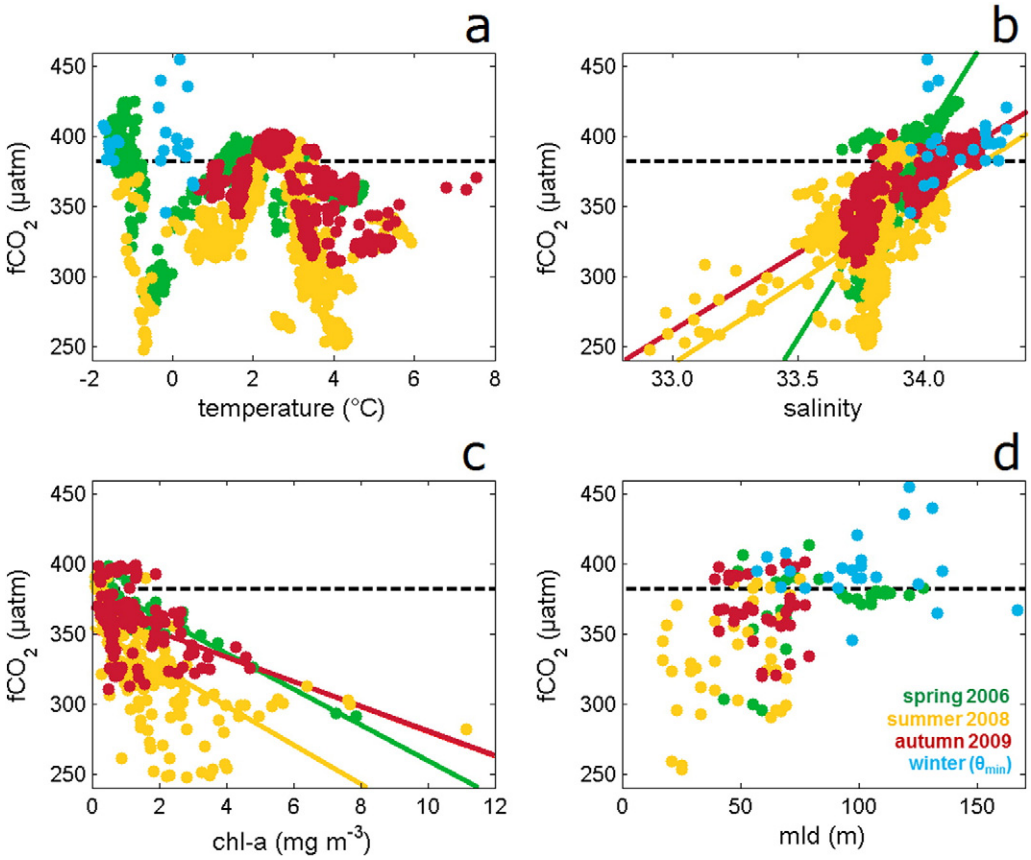

Fig. 7. Seasonal variability of sea surface fCO_2 (μatm) as a function of (a) temperature (°C), (b) salinity, (c) chlorophyll-a (chl-a, mg m^{-3}) and (d) mixed layer depth (mld, m) in austral spring 2006, summer 2008, autumn 2009 and winter (θ_{min}). Regression lines are shown for significant correlations. The average fCO_2 in air for 2006–2009 is shown for reference (black dashed line) where data below the line represent oceanic CO_2 undersaturation.

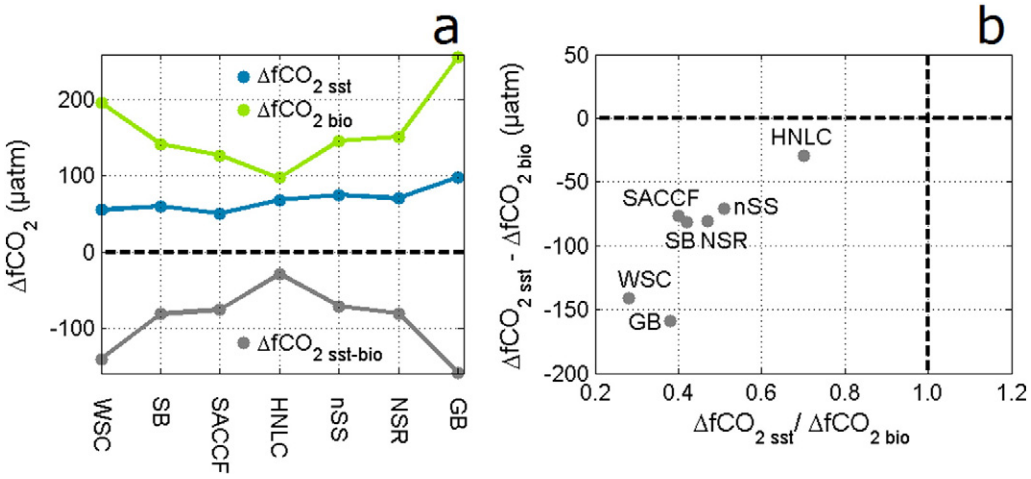

Fig. 8. Seasonal biological and temperature CO_2 signals, following Takahashi et al. (2002): (a) biological ($\Delta fCO_{2\ bio}$), temperature ($\Delta fCO_{2\ sst}$) and temperature–biological ($\Delta fCO_{2\ sst-bio}$) CO_2 disequilibrium as a mean per sub-region where zero ΔfCO_2 (black dashed line) marks the division between net seasonal CO_2 increase, above, and net seasonal CO_2 decrease, below; (b) CO_2 disequilibrium difference vs. ratio of temperature and biological signals as a mean per sub-region with the balance between both controls (zero ΔfCO_2 difference and ΔfCO_2 ratio of 1) marked by horizontal and vertical black dashed lines, respectively.

2012; Whitehouse et al., 2012) in the shallow surface waters, symptomatic of recent sea ice melt. The emergence of cryptophytes in the Weddell–Scotia Confluence and at the SB by the summer was indicative of a species shift from an ice edge diatom bloom (Jacques and Panouse, 1991; Buma et al., 1992; Korb et al., 2012).

Bloom development in the Weddell–Scotia Confluence and southern Scotia Sea is affected by the start and rate of sea ice retreat (Comiso et al., 1993; Korb et al., 2005; Murphy et al., 2007). During winter–spring 2006, sea ice reached its maximum northward extent at 57°S in August. Sea ice retreat began in September, exposing a large part of the SIZ to increased light levels and a meltwater stabilised water column potentially fertilised by iron and sea ice algae. Subsequently, a large bloom had developed by October 2006, which was identified as the strongest Scotia Sea bloom during the 3 year study period, accompanied by the negative CO_2 disequilibrium in the region of the SACCF and SB (Fig. 5). The intense bloom of spring–summer season 2006/7 was the strongest bloom of the entire region from 2006–2009 (Figs. 2 and 3) where the 'plume-like' structure of the bloom largely followed the course of the SACCF. High primary productivity drove the CO_2 undersaturation in the springtime diatom-dominated bloom (Korb et al., 2012), which then shifted to CO_2 saturation in a decaying bloom. The years 2007 and 2008 represented high and low wintertime sea ice extent during the study period, respectively, both with patchy and short-lived blooms in the SIZ after ice melt. This demonstrates the influence of sea ice on the biological activity of the Scotia Sea and contributed to large variations in bloom features in spring and summer. Large interannual variability in phytoplankton blooms in the Scotia Sea is imprinted on the seasonality observed during the spring, summer and autumn transects, i.e., bloom areal coverage ranged from 41,000 to 463,000 km^2 during the spring–summer season in different years across the Scotia Sea (Table 1). This is reflected in the year-to-year variability in marine productivity during the growing season (Constable et al., 2003; Smith and Comiso, 2008; Park et al., 2010; Korb et al., 2012). When present, blooms are regularly co-located to the broad position of the SACCF, which is visible to some extent during most spring seasons as a band extending west–east across the Scotia Sea (Fig. 2). The location-range of the SACCF from all three cruises was close to the northern most extent of the SIZ at 57°S and about 700 km downstream of the Antarctic Peninsula (Venables et al., 2012). Mesoscale activity associated with the SACCF was evident from variability in silicic acid during autumn (Venables et al., 2012; Whitehouse et al., 2012). Sea ice retreat occurred relatively late in October 2006 but by November 2006 had reached comparable extent to the other years. Following such rapid ice retreat, optimal light conditions and iron supply from an upstream source (perhaps in an episodic manner related to mesoscale activity) presented favourable conditions for sporadic blooms, such as that observed in spring–summer 2006/7. This is supported by the shift from productive diatom blooms with chlorophyll-a values greater than 7 mg m^{-3} and subsequent springtime CO_2 disequilibrium minimum of −80 µatm, to unproductive dinoflagellate communities (Korb et al., 2012) and fCO_2 saturated, warmer waters in the summer and autumn. Years of reduced sea ice cover (e.g., 2008) are exposed to more wintertime wind-driven mixing and possible enhanced outgassing of CO_2. Greater seasonal warming is likely to occur on the open sea surface and hence a larger temperature control is expected. Conversely, in icy years (e.g., 2007) where the seasonal temperature control is dampened through sea ice cover, comparatively greater ice edge perimeter could enhance bloom formation events upon sea ice melt, under favourable iron and light conditions, tipping the balance to larger biological control.

The magnitude of seasonal biological ($\Delta fCO_{2\ bio}$) and temperature ($\Delta fCO_{2\ sst}$) effects is further depicted by considering the difference between and respective ratio of $\Delta fCO_{2\ sst}$ and $\Delta fCO_{2\ bio}$, revealing that seasonal changes in oceanic fCO_2 in the Weddell–Scotia Confluence are substantial and highly variable (Fig. 8b). Despite large year to year variability, the blooms that develop in the wake of sea ice retreat exert a strong biological control on oceanic CO_2 in the Weddell–Scotia Confluence to generate one of the largest seasonal amplitudes in CO_2 disequilibrium in the Scotia Sea region.

4.2. Transient CO_2 uptake in the central Scotia Sea: sporadic blooms and HNLC waters

The central Scotia Sea displayed typical HNLC conditions, with the exception of a spring bloom in 2006, and had the lowest seasonal change in sea surface fCO_2 ($\Delta fCO_{2\ sst-bio}$ of −29 µatm). This region displayed the weakest biological control on oceanic CO_2 of 97 µatm, compensated by moderate temperature control of 68 µatm. Sea surface fCO_2 remained close to the atmospheric value in summer and autumn and reached supersaturation during the winter. Chlorophyll-a concentrations were less than 0.2 mg m^{-3} with a resident dinoflagellate population (Korb et al., 2012) in summer and autumn. However, the large springtime phytoplankton bloom in 2006 that extended into the HNLC sub-region generated fCO_2 undersaturation. Thus, the region displays overall weak seasonality in oceanic CO_2 with predominantly HNLC conditions. However, the presence of sporadic seasonal blooms influences the seasonal signal where biological carbon uptake becomes a strong

driver of oceanic CO_2, largely compensated by moderate temperature control.

4.3. Northern Scotia Sea: episodic CO_2 uptake superimposed on systematic CO_2 seasonal cycles

The northern Scotia Sea (nSS, NSR) exhibits a systematic seasonal cycle in CO_2 disequilibrium from (winter/spring) supersaturation to (summer) undersaturation to (autumn/winter) saturation. This is driven by large biological control ($\Delta fCO_{2\ bio}$) of 146–151 μatm, partially compensated by temperature effects ($\Delta fCO_{2\ sst}$) of 70–75 μatm. Maximum sea surface fCO_2 in deep mixed layers from winter to spring is reduced to a summertime fCO_2 minimum as biological production (chlorophyll-a) increases during the growing season.

Blooms in this region are variable, often building up biomass (chlorophyll-a) during spring, sometimes reaching a peak in summer and occasionally persisting until the autumn. Such fluctuations could be a result of seasonal iron depletion and/or re-supply, including inputs from interactions with the North Scotia Ridge and episodic iron enrichment events, i.e., Patagonian dust deposition (Erickson et al., 2003). In the established diatom bloom during summer 2008, the nSS–NSR subregions revealed distinct depletions in nitrate and phosphate (Korb et al., 2012; Whitehouse et al., 2012) as chlorophyll-a values reached 1.2 mg m^{-3}. This was accompanied by the observed seasonal shift in CO_2 disequilibrium from springtime (super)saturation into summertime undersaturation close to the North Scotia Ridge. By autumn, sea surface warming within a decaying diatom bloom and emergence of heterotrophic dinoflagellates (Korb et al., 2012) enabled sea surface fCO_2 to increase towards near saturation, demonstrating the temperature control in this region. The frequent blooms that develop by episodic events are superimposed on to seasonal warming, leading to little seasonality and overall net biological control in the northern Scotia Sea and across the North Scotia Ridge.

4.4. Substantial seasonal CO_2 uptake in the South Georgia bloom

Despite the highest wintertime sea surface fCO_2 values and strongest temperature control of the six sub-regions studied, substantial and sustained biological carbon uptake in the South Georgia bloom yielded very low sea surface fCO_2 from spring to summer to autumn, resulting in dominant biological control on oceanic CO_2 across the Georgia Basin (Fig. 8).

Wintertime maximum sea surface fCO_2 of up to 455 μatm in the Georgia Basin is the likely result of deep mixing, enabling CO_2-rich waters to permeate the winter mixed layer (Winter Water) (Jones et al., 2012). At this time, the sea surface reached fCO_2 supersaturation and was a potential strong source of CO_2 to the atmosphere. By the onset of spring, sea surface fCO_2 was reduced to near-saturation levels accompanied by moderate chlorophyll-a concentrations in the Georgia Basin. At this time the phytoplankton community was possibly light limited (heterotrophic dinoflagellates were dominant) and iron concentrations were low (Korb et al., 2012; Nielsdóttir et al., 2012). By summer, shallowing mixed layers and optimal light conditions were accompanied by peaks in chlorophyll-a concentrations of 11 mg m^{-3}, water column chlorophyll-a and rates of primary production (Korb et al., 2012). There was a shift in the phytoplankton community towards large diatoms. Waters were characterised by high surface iron concentrations exceeding 5 nM (Nielsdóttir et al., 2012) and a lack of phytoplankton response to iron addition experiments (Hinz et al., 2012); all indicative of an iron replete environment (Korb and Whitehouse, 2004; Korb et al., 2008). The sea surface reached a summertime minimum in CO_2 disequilibrium of −116 μatm that counteracted seasonal effects of sea surface warming. Substantial biological CO_2 uptake across the Georgia Basin created one of the strongest summertime sinks of 12.9 ± 11.7 mmol m^{-2} day^{-1} for atmospheric CO_2 and highest seasonal inorganic carbon depletion of 4.6 ± 0.8 mol m^{-2} in naturally iron fertilised ice-free waters of the Southern Ocean (Jones et al., 2012).

By the autumn, dinoflagellates had increased (Korb et al., 2012) and chlorophyll-a values still remained high. Respiration acted to slightly increase sea surface fCO_2. The northern part of the transect had the largest seasonal increase in sea surface temperature. The data showed a latitudinal increase in temperature control across the Scotia Sea region to a maximum $\Delta fCO_{2\ sst}$ of 98 μatm in the Georgia Basin. Considering the difference and ratio in seasonal ΔfCO_2 of biological and temperature effects, the phytoplankton blooms downstream (north) of South Georgia are strong, annual features that lead to dominant seasonal biological control of oceanic CO_2 of 257 μatm.

The annual occurrence of vast phytoplankton blooms downstream, to the north, of South Georgia is observed during the whole study period. High sea surface chlorophyll-a and productivity in this region have been previously documented (Korb and Whitehouse, 2004; Korb et al., 2008; Borrione and Schlitzer, 2013). Based on bloom area and duration, the longest lived, widespread blooms in the Georgia Basin occurred during the summer seasons and represented some of the strongest blooms in the wider Scotia Sea region from 2006 to 2009 (Table 1). These blooms often start during early spring, persisting until the autumn and regularly spread across the whole Georgia Basin. The areal limits of the bloom are strongly correlated to the contours of sea surface dynamic height (Venables et al., 2012), which can be seen by enhanced chlorophyll-a plumes within the jets of the SACCF and the PF to the south and north of the basin, respectively (Figs. 1 and 2).

The maximum areal extent of the South Georgia bloom in summer 2007/8 was determined as 325,000 km^2 (rank 2) and was the strongest South Georgia bloom from the 2006–2009 study period (Table 1). The presence of weakly and strongly silicified diatoms in sediment traps from 2000 m depth in the Georgia Basin suggest that there is a high particulate flux of organic carbon to depth (Korb et al., 2010, 2012; Whitehouse et al., 2012) and that the South Georgia bloom is another naturally iron fertilised hotspot of carbon export to the deep Southern Ocean. The blooms of summer seasons 2005/6, 2006/7, and 2008/9 are of similar duration and extent (Fig. 3) and therefore it can be inferred that, based on observations during a 'typical' summer, the South Georgia bloom creates considerable atmospheric CO_2 uptake and concomitant sequestration of organic carbon to depth and exerts a strong biological control on the annual cycle of oceanic CO_2.

4.5. Biological processes drive seasonal signals in oceanic CO_2 across the Scotia Sea

The new seasonally-resolved time series in oceanic CO_2 has allowed, for the first time, an assessment of the relative contribution of biological and temperature effects that drive the variability in oceanic CO_2 across the Scotia Sea region from spring to summer, autumn and winter. The seasonal basin-wide biological effect on oceanic CO_2, determined as the mean of $\Delta fCO_{2\ bio}$ for all sub-regions, is 159 μatm. The mean temperature effect ($\Delta fCO_{2\ sst}$) of 68 μatm partly (43%) compensates the biological control. This demonstrates the dominance of seasonal biological processes on oceanic CO_2 from the seasonal ice zone to the Polar Front. The relationship developed by Takahashi et al. (2002) to distinguish temperature and biological signals in sea surface fCO_2 (2) assigns all non-thermodynamic controls to biological processes. Subsequently, air–sea CO_2 exchange, advection, mixing, upwelling, calcification and carbonate dissolution are incorporated into the seasonal 'biological' signal. Uncertainties in the derived temperature and biological signals exist if the seasonal sea surface fCO_2 maxima and minima occur at finer temporal scales or at other locations than the seasonal meridional transects, which could be possible for the Scotia Sea, which has large spatial variability (as demonstrated by satellite imagery). However, the combination of (a) quasi-continuous sea surface fCO_2, temperature and salinity data; (b) frequent chlorophyll-a (Korb et al., 2012) and macronutrient (Whitehouse et al., 2012) measurements; and (c) regular hydrographic stations from spring (October–

November) 2006 to summer (January–February) to autumn (April–May) 2009 and the inclusion of winter (August–September) 2007 data from summer potential temperature minimum during this study provides sufficient spatio-temporal coverage to elucidate the main physical and biological controls on CO_2 disequilibrium in the Scotia Sea.

5. Conclusion

A first seasonally-resolved time series of oceanic CO_2 quantifies the effects of biological processes and temperature as drivers of the seasonal CO_2 cycle in the Scotia Sea. Spring, summer, autumn and winter fCO_2 data along a 1000 km meridional transect show that biological effects dominate temperature effects to control the seasonal signal of sea surface fCO_2. The naturally iron fertilised phytoplankton blooms that develop downstream (north) of the island of South Georgia each year promote substantial CO_2 uptake from spring to autumn. Despite wintertime CO_2 supersaturation and compensating temperature controls, the South Georgia blooms generate the largest seasonal fCO_2 amplitude for the entire Scotia Sea region. The seasonal ice zone was characterised by a large seasonal biological control and a weak temperature control. Strong seasonality in the presence of sea ice and phytoplankton blooms displayed a synergy with oceanic CO_2 in spring and summer. Ice-covered, CO_2-rich waters were swiftly transformed to regions of large CO_2 undersaturation as biological carbon uptake rapidly reduced the winter CO_2 reserve following sea ice melt. Oceanic CO_2 varied significantly with chlorophyll-a concentrations and sea ice cover, as strong CO_2 disequilibrium tracked the southward retreating ice edge. The weakest seasonal biological signal occurred in high-nutrient low-chlorophyll and CO_2-saturated waters of the central Scotia Sea. At the basin scale, biological processes exceeded temperature effects from the seasonal ice zone up to the Polar Front. The highly productive areas of the Scotia Sea region generate seasonally strong biological uptake of atmospheric CO_2 in the Southern Ocean.

Acknowledgements

The authors extend great thanks to the British Antarctic Survey and the DISCOVERY-2010 programme, the Captain, officers, crew and scientists onboard RRS *James Clark Ross* during cruises JR161, JR177 and JR200. Special thanks to Ian Brown and Gerald Moore, Plymouth Marine Laboratory, and the British Antarctic Survey for continual support of the CO_2 instrument and to Andy Watson and Mario Hoppema for insightful discussions and comments that helped in preparing the manuscript. Supporting data and statistical and practical advice were gratefully received from Rebecca Korb, Min Gordon, Michiel de Roo, Geraint Tarling, Angus Atkinson and Sophie Fielding. NASA, the SeaWiFS/MODIS programme and OSTIA at GHRSST are acknowledged for satellite data. Financial support was given by a NERC PhD studentship to EMJ (NER/F14/G6/115), under the auspices of the Centre for observation of Air–Sea Interactions and fluXes (CASIX) and the Antarctic Funding Initiative (CGS8/28).

References

Ardelan, M.V., Holm-Hansen, O., Hewes, C.D., Reiss, C.S., Silva, N.S., Dulaiova, H., Steinnes, E., Sakshaug, E., 2010. Natural iron enrichment around the Antarctic Peninsula in the Southern Ocean. Biogeosciences 7, 11–25. http://dx.doi.org/10.5194/bg-7-11-2010.

Atkinson, A., Whitehouse, M.J., Priddle, J., Cripps, G.C., Ward, P., Brandon, M.A., 2001. South Georgia, Antarctica: a productive, cold water, pelagic ecosystem. Mar. Ecol. Prog. Ser. 216, 279–308.

Bakker, D.C.E., Hoppema, M., Schroder, M., Geibert, W., de Baar, H.J.W., 2008. A rapid transition from ice covered CO_2-rich waters to a biologically mediated CO_2 sink in the eastern Weddell Gyre. Biogeosciences 5, 1373–1386.

Boehme, L., Meredith, M.P., Thorpe, S.E., Biuw, M., Fedak, M., 2008. Antarctic Circumpolar Current frontal system in the South Atlantic: monitoring using merged Argo and animal-borne sensor data. J. Geophys. Res. 113 (C09012). http://dx.doi.org/10.1029/2007JC004647.

Borrione, I., Schlitzer, R., 2013. Distribution and recurrence of phytoplankton blooms around South Georgia, Southern Ocean. Biogeosciences 10, 217–231. http://dx.doi.org/10.5194/bg-10-217-2013.

Boyd, P.W., Jickells, T., Law, C.S., Blain, S., Boyle, E.A., Buesseler, K.O., Coale, K.H., Cullen, J.J., de Baar, H.J.W., Follows, M., Harvey, M., Lancelot, C., Levasseur, M., Owens, N.P.J., Pollard, R.T., Rivkin, R., Sarmiento, J., Schoemann, V., Smetacek, V., Takeda, S., Tsuda, A., Turner, S., Watson, A.J., 2007. Mesoscale iron enrichment experiments 1993–2005: synthesis and future directions. Science 315, 612–617. http://dx.doi.org/10.1126/science.1131669.

Brainerd, K.E., Gregg, M.C., 1995. Surface mixed and mixing layer depths. Deep-Sea Res. I 42, 1521–1543. http://dx.doi.org/10.1016/0967-0637(95)00068-H.

Buma, A.G.J., Gieskes, W.W.C., Thomsen, H.A., 1992. Abundance of cryptophyceae and chlorophyll b containing organisms in the Weddell–Scotia Confluence area in the spring of 1988. Polar Biol. 12, 43–52. http://dx.doi.org/10.1007/BF00239964.

Comiso, J.C., McClain, C.R., Sullivan, C.W., Ryan, J.P., Leonard, C.L., 1993. Coastal zone color scanner pigment concentrations in the Southern-Ocean and relationships to geophysical surface-features. J. Geophys. Res. Oceans 98, 2419–2451. http://dx.doi.org/10.1029/92JC02505.

Constable, A.J., Nicol, S., Strutton, P.G., 2003. Southern Ocean productivity in relation to spatial and temporal variation in the physical environment. J. Geophys. Res. 108 (C4), 8079. http://dx.doi.org/10.1029/2001JC001270.

Cooper, D.J., Watson, A.J., Ling, R.D., 1998. Variation of pCO_2 along a North Atlantic shipping route (U.K. to the Caribbean): a year of automated observations. Mar. Chem. 60, 147–164. http://dx.doi.org/10.1016/S0304-4203(97)00082-0.

de Baar, H.J.W., de Jong, J.T.M., 2001. Distribution, sources and sinks of iron in seawater. In: Turner, D., Hunter, K. (Eds.), The Biogeochemistry of Iron in Seawater. Wiley, New York, pp. 123–253.

de Baar, H.J.W., Jong, J.T.M., Bakker, D.C.E., Löscher, B.M., Veth, C., Bathmann, U., 1995. Importance of iron for plankton blooms and carbon dioxide drawdown in the Southern Ocean. Nature 373, 412–415. http://dx.doi.org/10.1038/373412a0.

Dickson, A.G., Millero, F.J., 1987. A comparison of the equilibrium constants for the dissociation of carbonic acid in seawater media. Deep-Sea Res. 34, 1733–1743.

Dulaiova, H., Ardelan, M.V., Henderson, P.B., Charette, M.A., 2009. Shelf-derived iron inputs drive biological productivity in the southern Drake Passage. Glob. Biogeochem. Cycles 23. http://dx.doi.org/10.1029/2008GB003406.

Erickson III, D.J., Hernandez, J.L., Ginoux, P., Gregg, W.W., McClain, C., 2003. Atmospheric iron delivery and surface ocean biological activity in the Southern Ocean and Patagonian region. Geophys. Res. Lett. 30. http://dx.doi.org/10.1029/2003GL017241.

Feldman, G.C., McClain, C.R., 2006a. Ocean color web. In: Kuring, N., Bailey, S.W. (Eds.), MODIS Reprocessing 1.1. NASA Goddard Space Flight Center.

Feldman, G.C., McClain, C.R., 2006b. Ocean color web. In: Kuring, N., Bailey, S.W. (Eds.), SeaWiFS Reprocessing 5.1. NASA Goddard Space Flight Center.

GEBCO, 2001. General Bathymetric Chart of the Oceans Digital Atlas. British Oceanographic Data Centre, Liverpool, U.K.

Hardman-Mountford, N.J., Moore, G., Bakker, D.C.E., Watson, A.J., Schuster, U., Barciela, R., Hines, A., Moncoiffé, G., Brown, J., Dye, S., Blackford, J., Somerfield, P.J., Holt, J., Hydes, D.J., Aitken, J., 2008. An operational monitoring system to provide indicators of CO_2-related variables in the ocean. ICES J. Mar. Sci. 65, 1498–1503. http://dx.doi.org/10.1093/icesjms/fsn110.

Hewes, C.D., Reiss, C.S., Kahru, M., Mitchell, B.G., Holm-Hansen, O., 2008. Control of phytoplankton biomass by dilution and mixed layer depth in the western Weddell–Scotia Confluence. Mar. Ecol. Prog. Ser. 366, 15–29. http://dx.doi.org/10.3354/meps07515.

Hinz, D.J., Nielsdóttir, M.C., Korb, R.E., Whitehouse, M.J., Poulton, A.J., Moore, C.M., Achterberg, E.P., Bibby, T.S., 2012. Responses of microplankton community structure to iron addition in the Scotia Sea. Deep-Sea Res. II 59–60, 36–46. http://dx.doi.org/10.1016/j.dsr2.2011.08.006.

Holeton, C.L., Nédélec, F., Sanders, R., Brown, L., Moore, C.M., Stevens, D.P., Heywood, K.J., Statham, P.J., Lucas, C.H., 2005. Physiological state of phytoplankton communities in the southwest Atlantic sector of the Southern Ocean, as measured by fast repetition rate fluorometry. Polar Biol. 29, 44–52. http://dx.doi.org/10.1007/s00300-005-0028-y.

Holm-Hansen, O., Naganobu, M., Kawaguchi, S., Kameda, T., Krasovski, I., Tchernyshkov, P., Priddle, J., Korb, R., Brandon, M., Demer, D., Hewitt, R.P., Kahru, M., Hewes, C.D., 2004. Factors influencing the distribution, biomass, and productivity of phytoplankton in the Scotia Sea and adjoining waters. Deep-Sea Res. II 51, 1333–1350. http://dx.doi.org/10.1016/j.dsr2.2004.06.015.

Jacques, G., Panouse, M., 1991. Biomass and composition of size fractionated phytoplankton in the Weddell–Scotia Confluence area. Polar Biol. 11, 315–328. http://dx.doi.org/10.1007/BF00239024.

Jennings, J.C., Gordon, L.I., Nelson, D.M., 1984. Nutrient depletion indicates high primary productivity in the Weddell Sea. Nature 309, 51–54.

Jones, E.M., 2010. The Marine Carbon Cycle of the Scotia Sea, Southern Ocean Ph.D. Thesis, University of East Anglia (UEA e-prints).

Jones, E.M., Bakker, D.C.E., Venables, H.J., Whitehouse, M.J., Korb, R.E., Watson, A.J., 2010. Rapid changes in surface water carbonate chemistry during Antarctic sea ice melt. Tellus 62B, 621–635. http://dx.doi.org/10.1111/j.1600-0889.2010.00496.x.

Jones, E.M., Bakker, D.C.E., Venables, H.J., Watson, A.J., 2012. Dynamic seasonal cycling of inorganic carbon downstream of South Georgia, Southern Ocean. Deep-Sea Res. II 59–60, 25–35. http://dx.doi.org/10.1016/j.dsr2.2011.08.001.

Jullion, L., Naveira Garabato, A.C., Bacon, S., Meredith, M.P., Brown, P.J., Torres-Valdés, S., Speer, K.G., Holland, P.R., Dong, J., Bakker, D.C.E., Hoppema, M., Loose, B., Venables, H.J., Jenkins, W.J., Messias, M.-J., Fahrbach, E., 2014. The contribution of the Weddell Gyre to the lower limb of the Global Overturning Circulation. J. Geophys. Res. Oceans 119, 3357–3377. http://dx.doi.org/10.1002/2013JC009725.

Korb, R.E., Whitehouse, M.J., 2004. Contrasting primary production regimes around South Georgia, Southern Ocean: large blooms versus high nutrient, low chlorophyll waters. Deep-Sea Res. I 51, 721–738. http://dx.doi.org/10.1016/j.dsr.2004.02.006.

Korb, R.E., Whitehouse, M.J., Thorpe, S.E., Gordon, M., 2005. Primary production across the Scotia Sea in relation to the physico-chemical environment. J. Mar. Syst. 57, 231–249. http://dx.doi.org/10.1016/j.jmarsys.2005.04.009.

Korb, R.E., Whitehouse, M.J., Atkinson, A., Thorpe, S.E., 2008. Magnitude and maintenance of the phytoplankton bloom at South Georgia: a naturally iron replete environment. Mar. Ecol. Prog. Ser. 368, 75–91. http://dx.doi.org/10.3354/meps07525.

Korb, R.E., Whitehouse, M.J., Gordon, M., Ward, P., Poulton, A.J., 2010. Summer microplankton community structure across the Scotia Sea: implications for biological carbon export. Biogeosciences 7, 343–356. http://dx.doi.org/10.5194/bg-7-343-2010.

Korb, R.E., Whitehouse, M.J., Ward, P., Gordon, M., Venables, H.J., 2012. Regional and seasonal differences in microplankton biomass, productivity and structure across the Scotia Sea and implications to the export of biogenic carbon. Deep-Sea Res. II 59–60, 67–77. http://dx.doi.org/10.1016/j.dsr2.2011.06.006.

Lancelot, C., Mathot, S., Veth, C., de Baar, H.J.W., 1993. Factors controlling phytoplankton ice edge blooms in the Marginal Ice Zone of the northwestern Weddell Sea during sea ice retreat 1988 — field observations and mathematical modelling. Polar Biol. 13, 377–387. http://dx.doi.org/10.1007/BF01681979.

Landschützer, P., Gruber, N., Bakker, D.C.E., Schuster, U., 2014. Recent variability of the global ocean carbon sink. Glob. Biogeochem. Cycles 28, 927–949. http://dx.doi.org/10.1002/2014GB004853.

Lenton, A., Tilbrook, B., Law, R.M., Bakker, D.C.E., Doney, S.C., Gruber, N., Ishii, M., Hoppema, M., Lovenduski, N.S., Matear, R.J., McNeil, B.I., Metzl, N., Mikaloff Fletcher, S.E., Monteiro, P.M.S., Rödenbeck, C., Sweeney, C., Takahashi, T., 2013. Sea–air CO_2 fluxes in the Southern Ocean for the period 1990–2009. Biogeosciences 10, 4037–4054. http://dx.doi.org/10.5194/bgd-10-285-2013.

Lewis, R.A., Wallace, D.W.R., 1998. CO2SYS-Program developed for the CO_2 system calculations. Carbon Dioxide Information and Analysis Centre. Report ORNL/CDIAC-105.

Locarnini, R.A., Whitworth, T., Nowlin, W.D., 1993. The importance of the Scotia Sea on the outflow of Weddell Sea Deep Water. J. Mar. Res. 51, 135–153. http://dx.doi.org/10.1357/0022240933223846.

Mehrbach, C., Culberson, C.H., Hawley, J.E., Pytkowicz, R.M., 1973. Measurement of the apparent dissociation constants of carbonic acid in seawater at atmospheric pressure. Limnol. Oceanogr. 18, 897–907.

Meredith, M.P., Watkins, J.L., Murphy, E.J., Cunningham, N.J., Wood, A.G., Korb, R.E., Whitehouse, M.J., Thorpe, S.E., Vivier, F., 2003. An anticyclonic circulation above the Northwest Georgia Rise. Geophys. Res. Lett. 30 (20), 3327–3342. http://dx.doi.org/10.1029/2003GL018039 (2061).

Meredith, M.P., Naveira Garabato, A.C., Gordon, A.L., Johnson, G.C., 2008. Evolution of the deep and bottom waters of the Scotia Sea, Southern Ocean, during 1995–2005. J. Clim. 21, 3327–3342. http://dx.doi.org/10.1175/2007JCLI2238.1.

Meskhidze, N., Nenes, A., Chameides, W.L., Luo, C., Mahowald, N., 2007. Atlantic Southern Ocean productivity: fertilization from above or below? Glob. Biogeochem. Cycles 21, GB2006. http://dx.doi.org/10.1029/2006GB002711.

Metzl, N., Brunet, C., Jabaud-Jan, A., Poisson, A., Schauer, B., 2006. Summer and winter air–sea CO_2 fluxes in the Southern Ocean. Deep-Sea Res. I 53, 1548–1563. http://dx.doi.org/10.1016/j.dsr.2006.07.006.

Millero, F.J., 1995. Thermodynamics of the carbon dioxide system in the Oceans. Geochim. Cosmochim. Acta 59, 661–677.

Murphy, E.J., Clarke, A., Symon, C., Priddle, J., 1995. Temporal variation in Antarctic sea-ice: analysis of a long-term fast-ice record rom the South-Orkney Islands. Deep-Sea Res. I 42, 1045–1062. http://dx.doi.org/10.1016/0967-0637(95)00057-D.

Murphy, E.J., Watkins, J., Trathan, P.N., Reid, K., Meredith, M.P., Thorpe, S.E., Johnson, N.M., Clarke, A., Tarling, G., Collins, M.A., Forcada, J., Shreece, R.S., Atkinson, A., Korb, R.E., Whitehouse, M.J., Ward, P., Rodhouse, P.G., Enderlein, P., Hirst, A.G., Martin, A.R., Hill, S.L., Staniland, I.J., Pond, D.W., Briggs, D.R., Cunningham, N.J., Fleming, A.H., 2007. Spatial and temporal operation of the Scotia Sea ecosystem: a review of large-scale links in a krill centred food web. Philos. Trans. R. Soc. B 362, 113–148. http://dx.doi.org/10.1098/rstb.2006.1957.

Naveira Garabato, A.C., Heywood, K.J., Stevens, D.P., 2002. Modification and pathways of Southern Ocean deep waters in the Scotia Sea. Deep-Sea Res. I 49, 681–705. http://dx.doi.org/10.1016/S0967-0637(01)00071-1.

Naveira Garabato, A.C., Polzin, K.L., King, B.A., Heywood, K.J., Visbeck, M., 2004. Widespread intense turbulent mixing in the Southern Ocean. Science 303, 210–213. http://dx.doi.org/10.1126/science.1090929.

Nielsdóttir, M.C., Bibby, T.S., Moore, C.M., Hinz, D.J., Sanders, R., Whitehouse, M.J., Korb, R.E., Achterberg, E.P., 2012. Seasonal and spatial dynamics of iron availability in the Scotia Sea. Mar. Chem. 130–131, 62–72. http://dx.doi.org/10.1016/j.marchem.2011.12.004.

Nomura, D., Inoue, H.Y., Yoyota, T., 2006. The effect of sea-ice growth on air–sea CO_2 flux in a tank experiment. Tellus 58B, 418–426. http://dx.doi.org/10.1111/j.1600-0889.2006.00204.x.

Orsi, A.H., Whitworth, T., Nowlin, W.D., 1995. On the meridional extent and fronts of the Antarctic Circumpolar Current. Deep-Sea Res. I 42, 641–673. http://dx.doi.org/10.1016/0967-0637(95)00021-W.

Park, J., Im-Sang, O., Hyun-Cheol, K., Sinjae, Y., 2010. Variability of SeaWiFs chlorophyll-a in the southwest Atlantic sector of the Southern Ocean: strong topographic effects and weak seasonality. Deep-Sea Res. I 57, 604–620. http://dx.doi.org/10.1016/j.dsr.2010.01.004.

Patterson, S.L., Sievers, H.A., 1980. The Weddell–Scotia Confluence. J. Phys. Oceanogr. 10, 1584–1610. http://dx.doi.org/10.1175/1520-0485(1980)010<1584:TWSC>2.0.CO;2.

Pollard, R.T., Lucas, M.I., Read, J.F., 2002. Physical controls on biogeochemical zonation in the Southern Ocean. Deep-Sea Res. II 49, 3289–3305. http://dx.doi.org/10.1016/S0967-0645(02)00084-X.

Pollard, R.T., Salter, I., Sanders, R.J., Lucas, M.I., Moore, C.M., Mills, R.A., Statham, P.J., Allen, J.T., Baker, A.R., Bakker, D.C.E., Charette, M.A., Fielding, S., Fones, G.R., French, M., Hickman, A.E., Holland, R.J., Hughes, J.A., Jickells, T.D., Lampitt, R.S., Morris, E.E., Nedelec, F.H., Nielsdottír, M., Planquette, H., Popova, E.E., Poulton, A.J., Read, J.F., Seeyave, S., Smith, T., Stinchcombe, M., Taylor, S., Thomalla, S., Venables, H.J., Williamson, R., Zubkov, M.V., 2009. Southern Ocean deep-water carbon export enhanced by natural iron fertilization. Nature 457, 577–581. http://dx.doi.org/10.1038/nature07716.

Rysgaard, S., Glud, R.N., Sejr, M.K., Bendtsen, J., Christensen, P.B., 2007. Inorganic carbon transport during sea ice growth and decay: a carbon pump in polar seas. J. Geophys. Res. 112. http://dx.doi.org/10.1029/2006JC003572.

Schlitzer, R., 2002. Carbon export fluxes in the Southern Ocean: results from inverse modelling and comparison with satellite based estimates. Deep-Sea Res. II 49, 1623–1644. http://dx.doi.org/10.1016/S0967-0645(02)00004-8.

Sedwick, P.N., DiTullio, G.R., 1997. Regulation of algal blooms in Antarctic shelf waters by the release of iron from melting sea ice. Geophys. Res. Lett. 24, 2515–2518. http://dx.doi.org/10.1029/97GL02596.

Shim, J., Kang, Y.C., Kim, D., Choi, S.-H., 2006. Distribution of net community production and surface pCO_2 in the Scotia Sea, Antarctica, during austral spring 2001. Mar. Chem. 101, 68–84. http://dx.doi.org/10.1016/j.marchem.2005.12.007.

Smith, W.O., Comiso, J.C., 2008. Influence of sea ice on primary productivity in the Southern Ocean: a satellite perspective. J. Geophys. Res. 113. http://dx.doi.org/10.1029/2007JC004251.

Smith, I.J., Stevens, D.P., Heywood, K.J., Meredith, M.P., 2010. The flow of the Antarctic Circumpolar Current over the North Scotia Ridge. Deep-Sea Res. I 57, 14–28. http://dx.doi.org/10.1016/j.dsr.2009.10.010.

Sokolov, S., Rintoul, S.R., 2007. On the relationship between fronts of the Antarctic Circumpolar Current and surface chlorophyll concentrations in the Southern Ocean. J. Geophys. Res. 112. http://dx.doi.org/10.1029/2006JC004072.

Stark, J.D., Donlon, C.J., Martin, M.J., McCulloch, M.E., 2007. OSTIA: an operational, high resolution, real time, global sea surface temperature analysis system. Marine Challenges: Coastline to Deep Sea. Conference Proceedings. Oceans '07 IEEE Aberdeen.

Takahashi, T., Olafsson, J., Goddard, J.G., Chipman, D.W., Sutherland, S.C., 1993. Seasonal variation of CO_2 and nutrients in the high latitude surface oceans — a comparative study. Glob. Biogeochem. Cycles 7, 843–878. http://dx.doi.org/10.1029/93GB02263.

Takahashi, T., Sutherland, S.C., Sweeney, C., Poisson, A., Metzl, N., Tilbrook, B., Bates, N., Wanninkhof, R., Feely, R.A., Sabine, C.L., Olafsson, J., Nojiri, Y., 2002. Global sea–air CO_2 flux based on climatological surface ocean pCO_2, and seasonal biological and temperature effects. Deep-Sea Res. II 49, 1601–1622. http://dx.doi.org/10.1016/S0967-0645(02)00003-6.

Takahashi, T., Sutherland, S.C., Wanninkhof, R., Sweeney, C., Feely, R.A., Chipman, D.W., Hales, B., Friederich, G., Chavez, F., Sabine, C.L., Watson, A.J., Bakker, D.C.E., Schuster, U., Metzl, Yoshikawa-Inoue, Ishii, H., Midorikawa, M., Nojiri, T., Körtzinger, Y., Steinhoff, T., Hoppema, M., Olafsson, J., Arnarson, T.S., Tilbrook, B., Johannessen, T., Olsen, A., Bellerby, R., Wong, C.S., Delille, B., Bates, N.R., de Baar, H.J.W., 2009. Climatological mean and decadal change in surface ocean pCO_2, and net sea–air CO_2 flux over the global oceans. Deep-Sea Res. II 56, 554–577. http://dx.doi.org/10.1016/j.dsr2.2008.12.009.

Tarling, G.A., Ward, P., Atkinson, A., Collins, M., Murphy, E.J., 2012. Editorial: discovery 2010: understanding the Scotia Sea food web. Deep-Sea Res. II 59–60, 1–13.

Thomas, H., Bozec, Y., Elkalay, K., de Baarm, H.J.W., Borges, A.V., Schiettecatte, L.-S., 2005. Controls of the surface water partial pressure of CO_2 in the North Sea. Biogeosciences 2, 323–334.

Thorpe, S.E., Heywood, K.J., Brandon, M.A., Stevens, D.P., 2002. Variability of the Southern Antarctic Circumpolar Current Front north of South Georgia. J. Mar. Syst. 37, 87–105. http://dx.doi.org/10.1016/S0924-7963(02)00197-5.

Trathan, P.N., Brandon, M.A., Murphy, E.J., Thorpe, S.E., 1997. Characterisation of the Antarctic Polar Frontal Zone to the north of South Georgia in summer 1984. J. Geophys. Res. 102, 10483–10497.

van Heuven, S., Pierrot, D., Rae, J.W.B., Lewis, E., Wallace, D.W.R., 2011. MATLAB program developed for CO_2 system calculations, ORNL/CDIAC-105b. Carbon Dioxide Int. Anal. Cent.Oak Ridge Natl. Lab., US DOE, Oak Ridge, Tenn

Venables, H.J., Meredith, M.P., Atkinson, A., Ward, P., 2012. Fronts and habitat zones in the Scotia Sea. Deep-Sea Res. II 59–60, 14–24. http://dx.doi.org/10.1016/j.dsr2.2011.08.012.

Watson, A.J., Orr, J.C., 2003. Carbon dioxide fluxes in the global ocean. In: Fasham, M.J.R. (Ed.), Ocean Biogeochemistry: The Role of the Ocean Carbon Cycle in Global Change. Springer-Verlag, Berlin.

Weiss, R.F., Price, B.A., 1980. Nitrous-oxide solubility in water and seawater. Mar. Chem. 8, 347–359. http://dx.doi.org/10.1016/0304-4203(80)90024-9.

Whitehouse, M.J., Korb, R.E., Atkinson, A., Thorpe, S.E., Gordon, M., 2008. Formation, transport and decay of an intense phytoplankton bloom within the high-nutrient low-chlorophyll belt of the Southern Ocean. J. Mar. Syst. 70, 150–167. http://dx.doi.org/10.1016/j.jmarsys.2007.05.003.

Whitehouse, M.J., Atkinson, A., Korb, R.E., Venables, H.J., Pond, D.W., Gordon, M., 2012. Substantial primary production in the land-remote region of the central and northern Scotia Sea. Deep-Sea Res. 59–60, 47–56. http://dx.doi.org/10.1016/j.dsr2.2011.05.010.

Whitworth, T., Nowlin, W.D., Orsi, A.H., Locarnini, R.A., Smith, S.G., 1994. Weddell Sea shelf water in the Bransfield Strait and Weddell–Scotia Confluence. Deep-Sea Res. I 41, 629–641. http://dx.doi.org/10.1016/0967-0637(94)90046-9.

Zhou, M., Zhu, Y., Dorland, R.D., Measures, C.I., 2010. Dynamics of the current system in the southern Drake Passage. Deep-Sea Res. I 57, 1039–1048. http://dx.doi.org/10.1016/j.dsr.2010.05.012.